EUROPEAN ORGANIZATION FOR NUCLEAR RESEARCH
CERN-AB DIVISION

CERN-AB-2003–094 (ABP)
Tevatron Beams-doc-535-v1

Losses of Protons During the Ramp

T.Sen*, F.Schmidt, R. Moore*, V. Shiltev*

Abstract

Beam losses during the ramp in the Tevatron are significant in both species. The losses in protons occur early in the ramp while anti-proton losses occur throughout the ramp. Furthermore the anti-proton losses are influenced by beam-beam effects while proton losses are relatively independent of these effects. We report on measurements and studies to explore the mechanisms behind the proton losses.

Fermi National Accelerator Laboratory, Batavia, Illinois, USA

AB/DIV Reps

Geneva, Switzerland

25 November, 2003

Proton losses during acceleration in the Tevatron

R. Moore, F. Schmidt*, T. Sen, V. Shiltsev

Reported by: T. Sen

March 28, 2003

1 Introduction

Beam losses on the Tevatron ramp have been significant since the beginning of Run II (March 1, 2001). In the last year they have become the most significant contributor to the Tevatron inefficiency. Losses on the ramp can not be attributed to a single effect. Several phenomena take place - e.g., losses due to shaving on a physical aperture, dynamic aperture (DA) effects due to machine nonlinearities, reduced DA due to beam-beam effects, loss of the DC beam, reduction of RF bucket area, etc. Figure 1 shows the variation of several parameters on the ramp in store 2328 (March 16, 2003, initial peak luminosity 40.6×10^{30} $\mathrm{cm}^{-2}\mathrm{s}^{-1}$).

The ramp takes about 84 seconds, during which the beam energy (blue curve) changes from 150GeV to 978GeV - first it follows a parabola, but goes linear after about 50 sec. The plot in Figure 1 covers about 80 sec before the ramp, ramp and about 80 seconds after the end of the ramp (at "flat top"). Black, green and blue lines represent proton bunched beam intensity FBIPNG (total in 36 bunches), antiproton bunched beam intensity FBIANG and total DC beam intensity in the Tev IBEAM, respectively, normalized to their values at 980 GeV, namely, FBIPNG=7650e9, FBIANG=945e9, IBEAM=9080e9. The proton losses take place before 400 GeV, in the the first 40 seconds and do not change after that. Because the proton intensity is about 8 times the antiproton one, the total beam intensity (IBEAM) follows the proton loss pattern except the very first few seconds when it loses 2% of the beam not captured by the RF system. The temporal distribution of the proton losses is much like the time dependence of the longitudinal bunch emittance - see magenta line in Figure 1 which represents relative changes of the quantity of $\sigma_s^2\sqrt{\gamma\sin\phi_s}$, where σ_s is the rms bunch length (SBDPSS) measured by sampled bunch display (SBD), and ϕ_s is the synchronous RF phase. Another indication of the dependence of the ramp losses on the longitudinal emittance is provided by store statistics - e.g., during 10 high energy physics stores in March 2003 (from # 2315 to # 2361), the proton ramp losses averaged around 3.4% in the five stores where 5-bunch coalescing in the main Injector was used, compared to average 7.0% proton losses in the stores with 7 bunches coalescing. According to the Tevatron SBD, longitudinal emittance of a proton bunch created after coalescing 7 MI bunches is about 35% larger than the 5-bunch coalescing emittance.

In order to prepare for the ramp, the Tevatron sequencer program increases vertical and horizontal chromaticities by several units about 20 seconds before the ramp and that leads

*Visitor from CERN

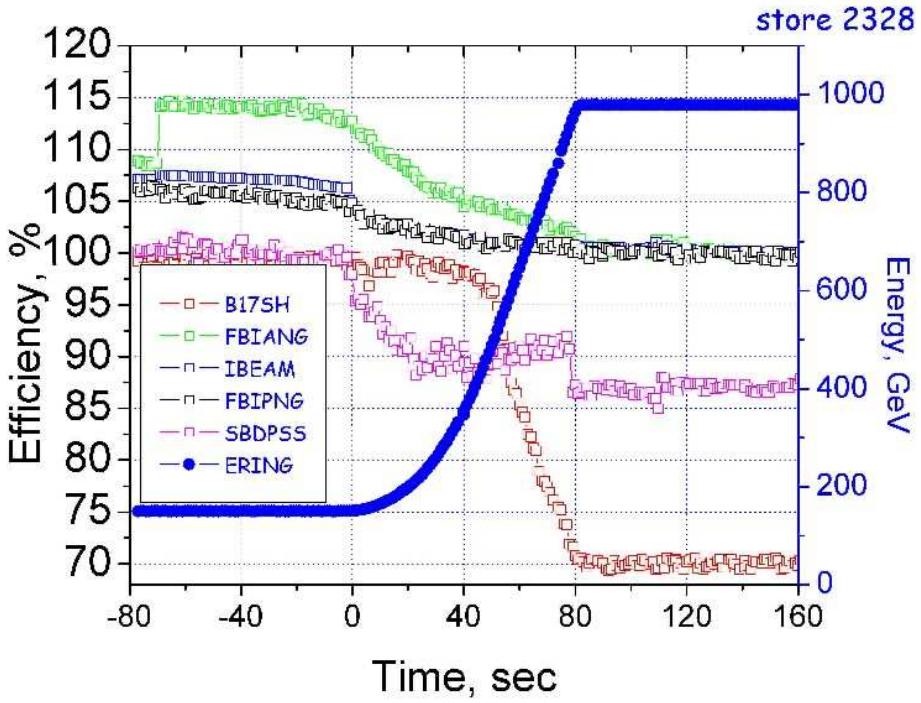

Figure 1: (color).Transfer efficiencies during the ramp in store 2328.

to some 2% pbar loss. The pbar intensity line has an obvious kink at 250 GeV or 30 seconds after start of the ramp - some 7% of antiprotons are lost before and 6% after that moment - and that is quite different from the proton loss distribution. That difference might be attributed to additional losses due to parasitic beam-beam interaction with high intensity proton bunches. For example, the red line in Figure 1 shows relative changes of the product $S = V_{B17}/\sqrt{\gamma}$ where V_{B17} is the voltage on one of the plates of the horizontal electrostatic separator installed at B17H. All the separators scale the same way on the ramp and one can see that effective beam-beam sepration S in units of the rms beam size is kept constant till about 500GeV (some 50 sec on ramp) and then gradually goes down by 30% at the end of the ramp.

Table 1 shows the severity of the beam losses since March 2002: One can see antiproton

	03/02	10/02	01/03	03/03
Protons/bunch	140e9	170e9	180e9	205e9
Pbars/bunch	7.5e9	22e9	20e9	23e9
P-loss at 150 GeV	23%	14%	16%	10%
Pbar-loss at 150 GeV	20%	9%	4%	4%
P-loss on ramp	7%	6%	9%	5%
Pbar-loss on ramp	14%	8%	12%	11%
Pbar-loss in squeeze	25%	5%	3%	2%

Table 1: Beam losses in the Tevatron at various stages before collisions are initiated.

and proton losses on the ramp together with proton losses at 150 GeV were and still are the dominant contributors in the Tevatron inefficiency. This motivated the need to better understand beam phenomena during the ramp.

Two dedicated experiments were done, the first in September 2002 and the second in January 2003 to identify the mechanisms that cause protons to be lost during the ramp. In both experiments, only proton bunches were injected and ramped. The conditions in the Booster and the Main Injector were adjusted so that the bunches had different intensities and emittances. The preparation of the bunches was different in the two experiments and they are described separately below. We report on the latest experiment first and the earlier experiment second.

In both these experiments we focused on how bunch parameters like emittances and intensities affect the loss during the ramp. Machine parameters such as the tunes, chromaticities and coupling also have strong influences on the loss. These have been studied several times by others and their values were chosen so as to minimize the losses. We will not address the dependence of losses on the machine parameters in this report.

2 Experiment of January 6, 2003

Our aim was to isolate the dependence of the loss during the ramp on the intensity, and the longitudinal emittance. The major part of the experiment involved preparing the bunches in the Main Injector. The number of bunches coalesced, the time at which the capturing lower frequency rf cavity is turned on and the number of Booster turns accumulated were all varied. We had also intended to isolate the dependence on the vertical emittance but time did not allow the preparation of these bunches.

In the first part of the experiment three groups of 9 bunches each were injected as follows:

- Group A: 9 control bunches (11 Booster turns, 5 coalesced bunches in MI) in P10 - P18. Coalescing adjusted to increase $\epsilon_s \approx 3$nsec
- Group B: 9 bunches (11 Booster turns, 5 coalesced bunches in MI) in P1 - P9. Coalescing optimized for lowest longitudinal $\epsilon_s \approx 2.3$nsec. Similar intensities as in Group A.
- Group C: 9 bunches - 7 bunches coalesced in MI with different numbers of Booster turns for intensities different from that in Group A. Desired similar longitudinal emittance as in Group A.
  - 11 Booster turns - P19-P21
  - 8 Booster turns - P22-P24
  - 6 Booster turns - P25-P27

The timing of the LLRF parameter to adjust the coalescing was the same for groups A and C but different for group B, hence group B was injected first. Pulse to pulse variations from the Booster and coalescing inefficiencies resulted in significant variations of bunch parameters within a group. It turned out to be impractical to control only one parameter at a time but we successfully injected bunches with a large range of variation in both intensity and longitudinal emittance. After injection the lifetime, transverse emittance and longitudinal profiles (using the SBD display provided by R. Flora and S. Pordes) of these

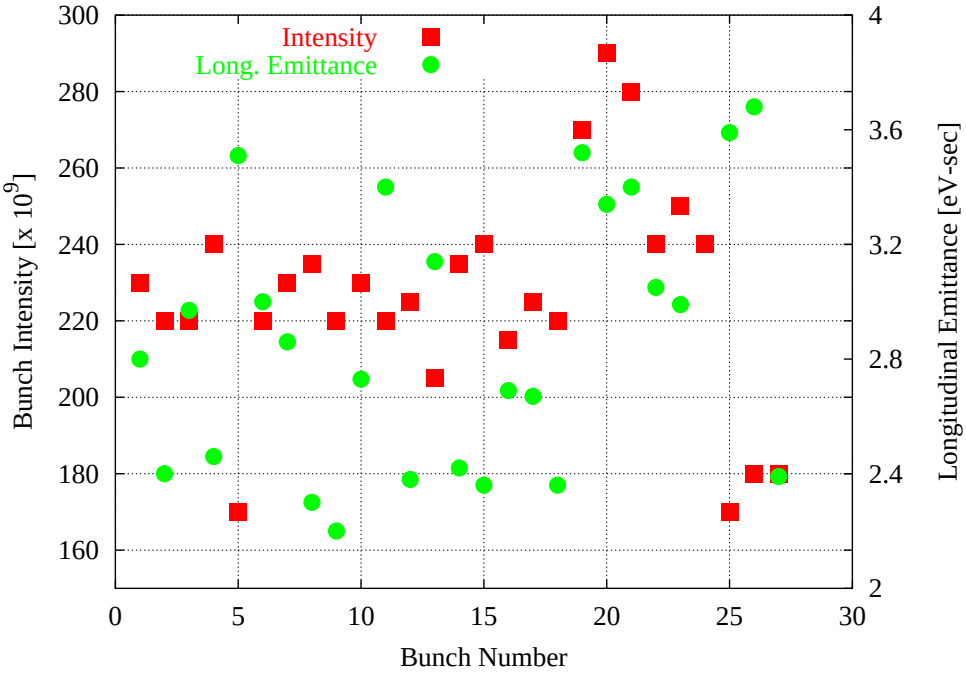

Figure 2.1: (color) Bunch intensity and longitudinal emittances as measured in the Main Injector vs bunch number.

bunches were measured first on the central orbit, then on the proton helix before ramping. After acceleration these measurements were repeated. At each stage the lifetime was recorded over an approximately 15 minute interval. During this experiment the longitudinal dampers were not active but transverse dampers were turned on. Figure 2.1 shows the bunch intensity and longitudinal emittances of the individual bunches as measured in the Main Injector.

The second part of the experiment investigated the losses while accelerating on the anti-proton helix. In the first attempt a proton bunch was injected directly onto the anti-proton helix as is done during anti-proton injection. This was a mistake. The bunch was moved in the opposite direction resulting in a quench. After recovery from the quench, the little time remaining allowed us to inject only two proton bunches:

- 1 "nominal" bunch (7 coalesced bunches, 11 Booster turns), P1
- 1 low intensity bunch (5 coalesced bunches, 4 Booster turns), P12. The aim was to have intensity and emittance similar to that of a typical anti-proton bunch.

These bunches were injected onto the central orbit, then moved to the anti-proton helix with the separator polarities reversed. The longitudinal profiles were measured on the central orbit and then again after acceleration on the anti-proton helix. During this part of the experiment, the transverse dampers were also turned off. The rationale was that the sequence of operations that turns on the transverse damper also lowers the chromaticity which could reduce the chromaticity on the anti-proton helix to negative values, hence driving the protons unstable.

In both experiments, the tunes were set to their nominal values (0.583, 0.575), the coupling corrected to a minimum tune split of 0.003 and the chromaticities to the nominal

values of 8 units in both planes.

2.1 Protons on the proton helix - analysis

From the data we calculated the proton lifetimes on the helix for individual proton bunches. Figure 2.2 shows the lifetime as a function of the bunch intensity (FBIPNG) and the bunch lengths (SBDPSS) - which are obtained as rms values from a Gaussian fit. Clearly the lifetime on the helix does not depend much on the bunch intensity. There is a clearer dependence of the lifetime on the initial bunch length. The rms values larger than 5 nsec indicate that these bunches are significantly non-Gaussian, as Gaussian bunches with $\sigma_s > 5$nsec would not fit within a 18nsec bucket. These very long bunches resulted from the non-optimized coalescing in the Main Injector.

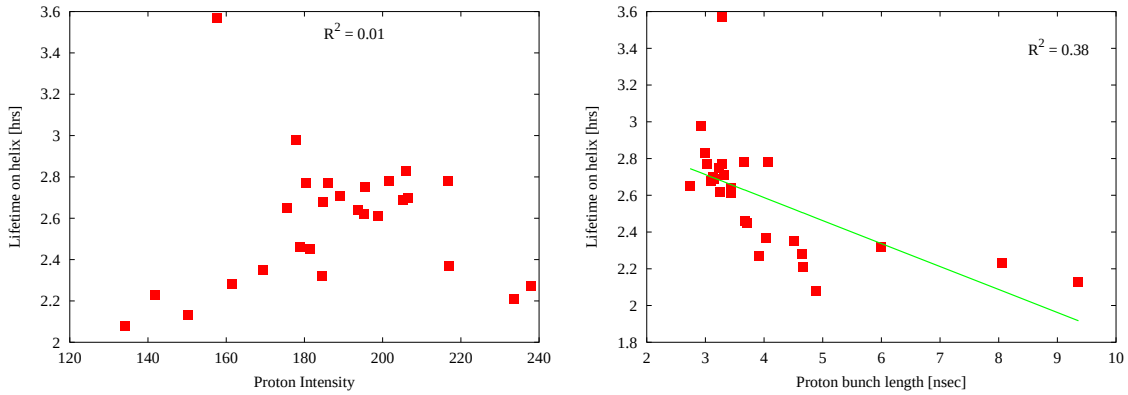

Figure 2.2: (color) Lifetime on the helix at 150 GeV. Left: vs bunch intensity, Right: vs bunch length (from SBDPSS). R^2 is the correlation coefficient.

As acceleration begins, there is a precipitous drop in the lifetime. Figure 2.3 shows the instantaneous lifetime $\tau = -N/dN/dt$ at the start of the ramp as a function of intensity and bunch length. This instantaneous lifetime also seems to be independent of the bunch intensity. The bunch length does influence the initial lifetime or loss rates but the correlation is not dramatic. *The unambiguous result however is that all long bunches suffer rapid loss at the start of the ramp.*

The ramp lasts a little longer than 80 seconds. Figure 2.4 shows the bunched beam intensity (FBIPNG) and the beam energy (ERING) during this portion of the study. The largest beam loss occurs during the initial part of the ramp. We zoom in on the longitudinal dynamics in this part of the ramp. The bucket area at the start of the ramp is about 4.3 eV-sec, then decreases for the first 10 seconds to a minimum around 4.0 eV-sec before increasing to a final value of 10.4 eV-sec at 977 GeV. Figure 2.5 shows the bucket area for the first 20 seconds of the ramp. The synchronous phase required for the area of an accelerating bucket is calculated from the energy (ERING) shown in Figure 2.4. It is evident that the energy data is not smooth during the ramp which results in a non-smooth bucket area. Therefore we have fitted the calculated area by a cubic polynomial curve in the least squares sense and the smoothed area curve is shown in Figure 2.5. Also shown in this figure is the smoothed beam intensity curve (also a cubic polynomial fit to the very noisy FBIPNG data shown in Figure 2.4) during this portion of the ramp. We observe that a large fraction of the beam loss occurs during the stage when the bucket area is decreasing. This is to be expected

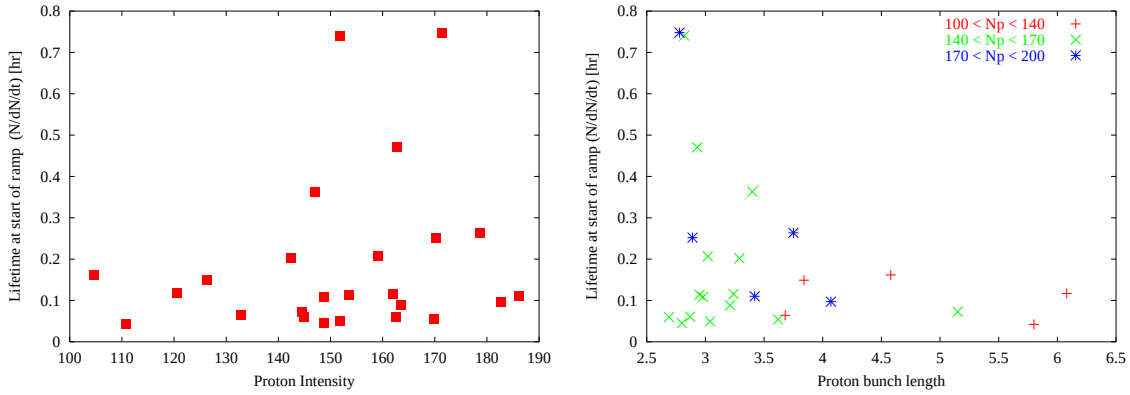

Figure 2.3: (color) Lifetime at the start of the ramp at 150 GeV. Left: vs bunch intensity, Right: vs bunch length (from SBDPSS).

since the bunches injected into the Tevatron are long and almost fill the bucket at 150 GeV. This suggests that changing the ramp parameters to increase the bucket area in the first 10 seconds may be helpful. Apparently one attempt last year at doing this was not successful and did not reduce the beam losses.

2.1.1 Bunch dependent losses on the ramp

The left plot in Figure 2.6 shows the losses on the ramp vs bunch number. There are no major differences in transmission loss between the three groups. The likely explanation is that the bunch parameters were not well controlled as intended due to the variability in Booster pulses and coalescing efficiencies in the Main Injector. Instead we will examine losses as a function of the bunch parameters. The right plot in Figure 2.6 shows that there is almost no dependence of the loss on the bunch intensity, the correlation coefficient $R^2 \sim 0$.

We have seen that the Gaussian rms values of the bunch length are very large for some bunches indicating that these bunches are very non-Gaussian. We have therefore calculated the rms values of the bunch length from the measured longitudinal density as follows [1]:

$$\begin{aligned} s_{rms} &= \left[\int s^2 \rho_N ds - (\int s \rho_N ds)^2\right]^{1/2} \\ \rho_N(s) &= \frac{1}{\int \rho ds}\rho(s) \end{aligned} \tag{1}$$

$\rho(s)$ is the measured longitudinal density profile while ρ_N is the normalized density. If the longitudinal profile were stationary, s_{rms} would be a good stationary measure of the bunch length. Unfortunately during this experiment the longitudinal dampers were off at 150 GeV so the "dancing" of the bunches was not damped at injection. Thus the profiles we captured did not represent the equilibrium bunch distribution. Nevertheless s_{rms} is likely to be a better measure of the bunch length than the Gaussian rms (which also uses the instantaneous profile) given the strongly non-Gaussian nature of the bunches.

[1] To remove unphysical large contributions to the rms values from the tails, we truncated the profile at the first zero crossing with the baseline

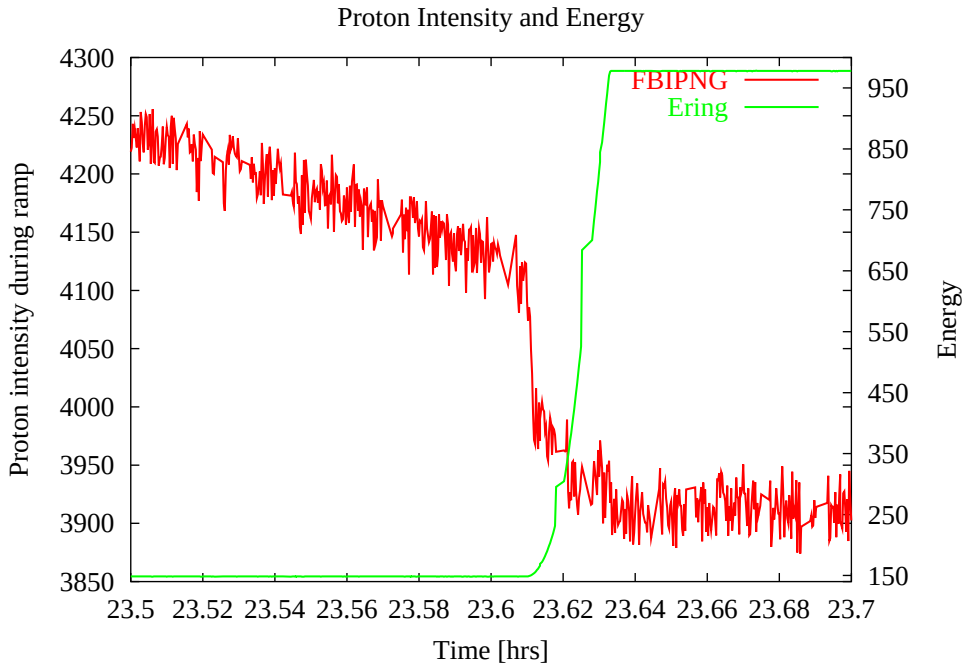

Figure 2.4: (color) Proton beam energy (ERING) and beam intensity (FBIPNG) during the study.

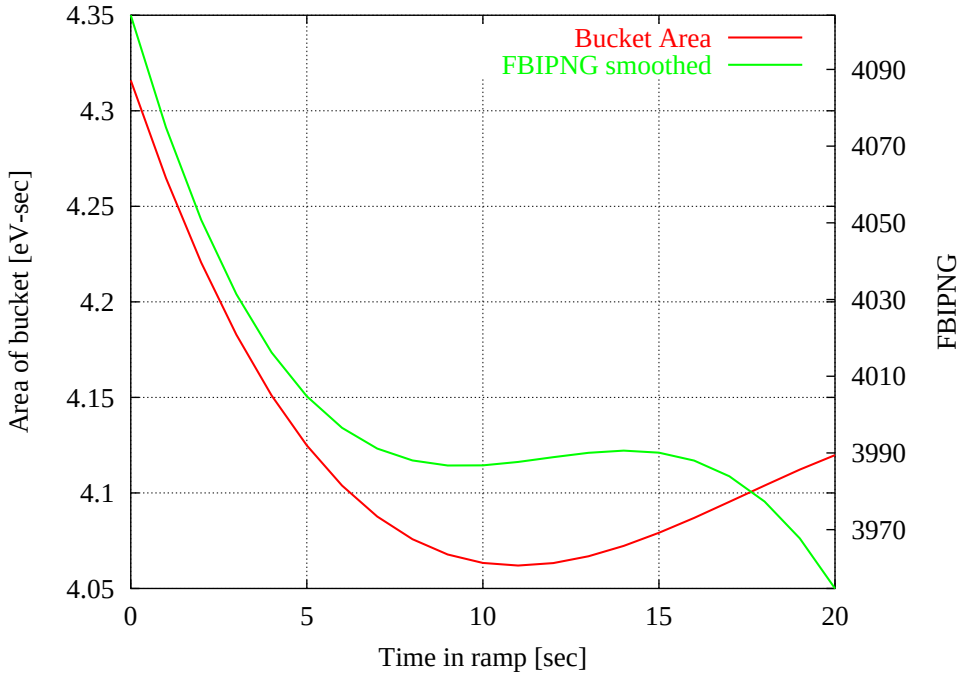

Figure 2.5: (color) The bucket area and the beam intensity during the initial stages of the ramp. These curves represent smoothed fits through the values at each second. Note that a large portion of the beam loss occurs while the bucket area is shrinking. See the text for a discussion.

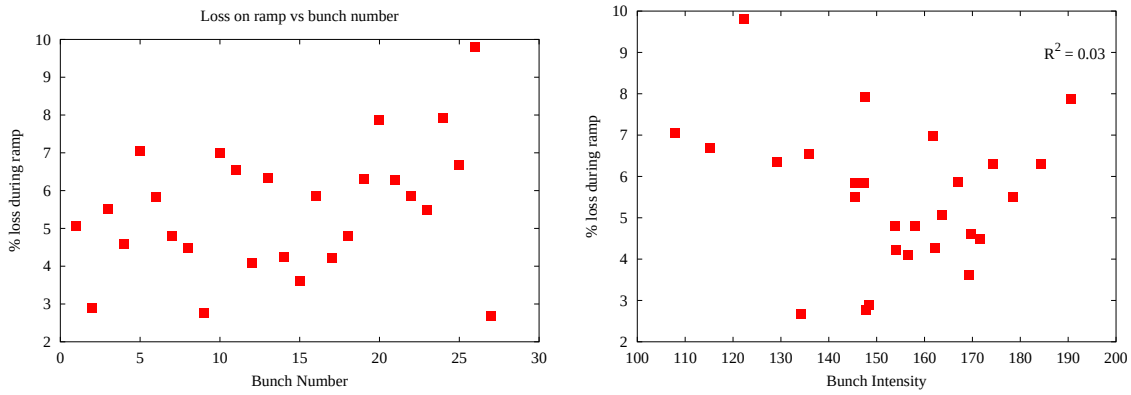

Figure 2.6: Ramp losses vs bunch number (left), vs bunch intensity (right)

Figure 2.7 shows the transmission loss as a function of the "true" rms s_{rms}. There is a strong correlation of the loss with the bunch length, with a correlation coefficient $R^2 = 0.6$. Figure 2.8 shows the correlation of the loss with the difference between the Gaussian rms and s_{rms}. The losses are greater than 6% for all bunches for which this difference exceeds 2 nsec. Combining the results of Figures 2.7 and 2.8 one can conclude that the transmission loss is greatest for all long bunches with non-Gaussian profiles.

We also examined the correlation of the loss with higher moments of the longitudinal density, the skewness and the kurtosis, defined as

$$\text{skewness} = \frac{\langle [s - \langle s \rangle]^3 \rangle}{s_{rms}^3}, \quad \text{kurtosis} = \frac{\langle [s - \langle s \rangle]^4 \rangle}{s_{rms}^4} - 3, \qquad \langle s^p \rangle \equiv \int s^p \rho_N ds \tag{2}$$

The skewness is a measure of the left-right asymmetry of the distribution; it is zero for a Gaussian distribution. The kurtosis is a measure of the "peakedness" of the distribution. It is zero for a Gaussian distribution, a negative value implies that the distribution is flatter than a Gaussian.

The left plot in Figure 2.9 shows that the loss is not very dependent on the skewness. Given the fact that the bunches are sloshing around in the bucket, the skewness or asymmetry is time dependent anyhow. The right plot in Figure 2.9 shows that the loss does increase as the kurtosis becomes more negative or deviates more from a Gaussian. The correlation coefficient of the loss with the kurtosis is a non-negligible $R^2 = 0.34$.

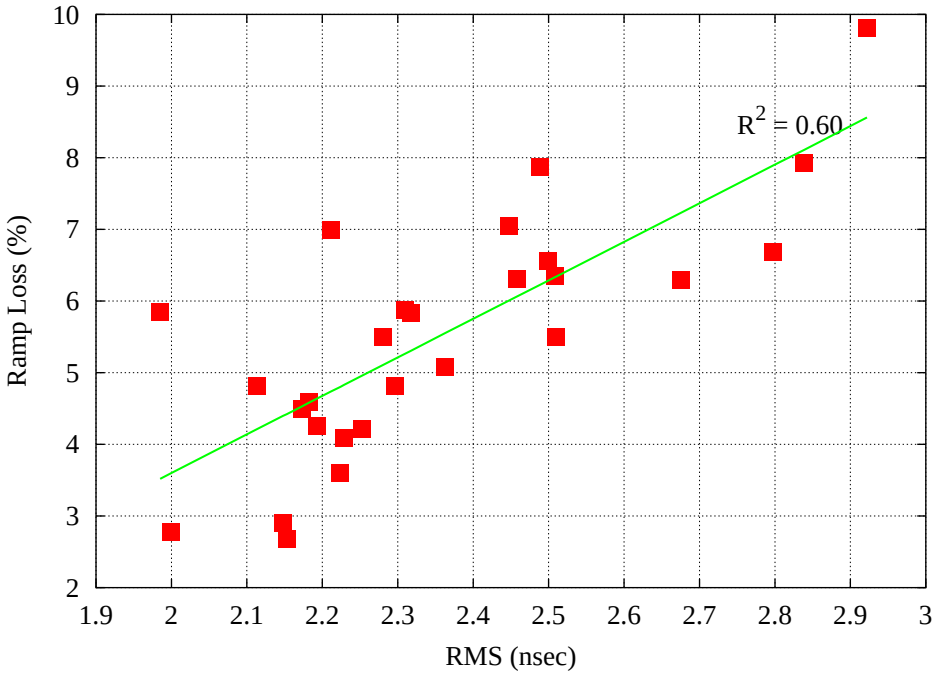

Figure 2.7: Loss as a function of the "true" rms bunch length s_{rms} defined in Equation (1).

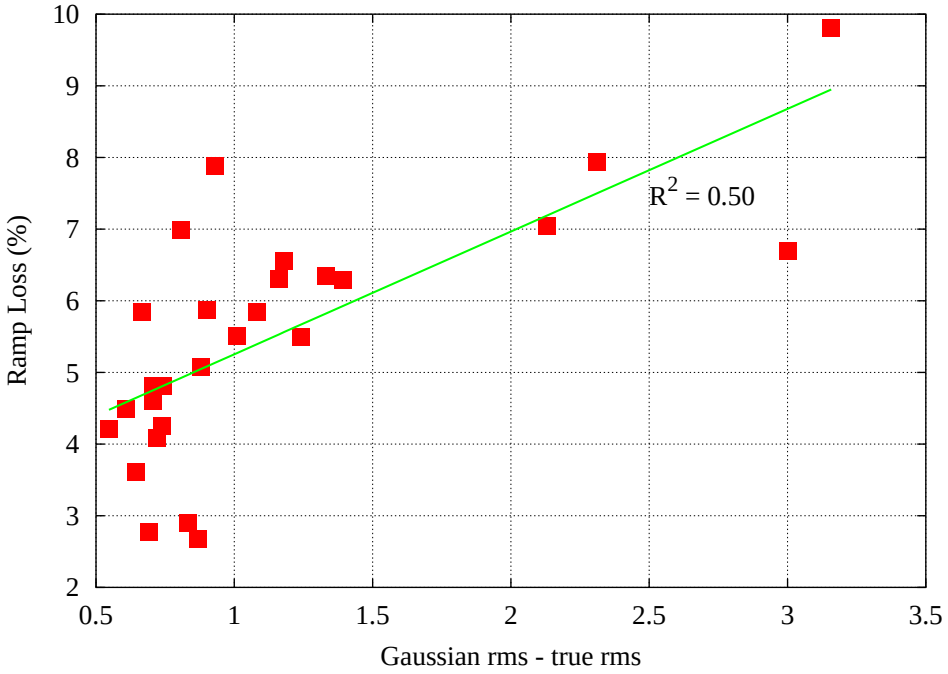

Figure 2.8: Ramp loss vs the difference between the Gaussian rms and the "true" rms as defined in Equation (1).

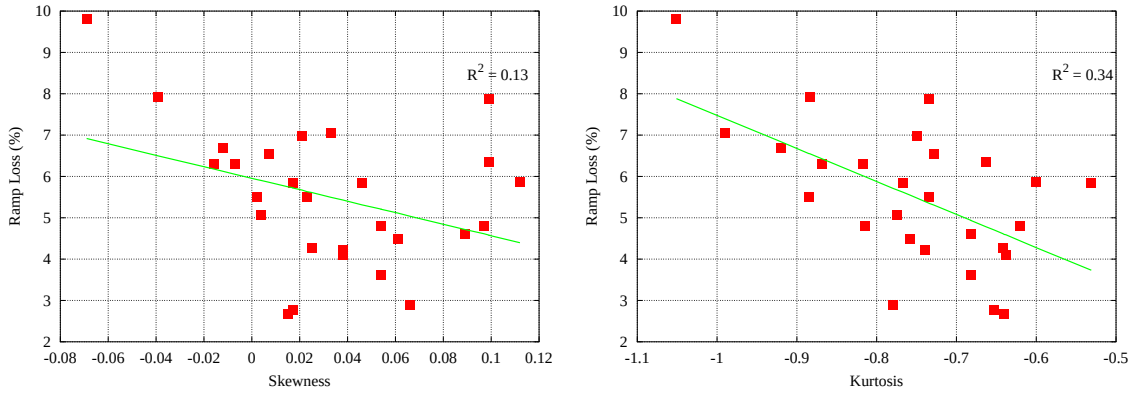

Figure 2.9: Loss as a function of the higher order moments of the longitudinal density. Left: vs the skewness, Right: vs the kurtosis.

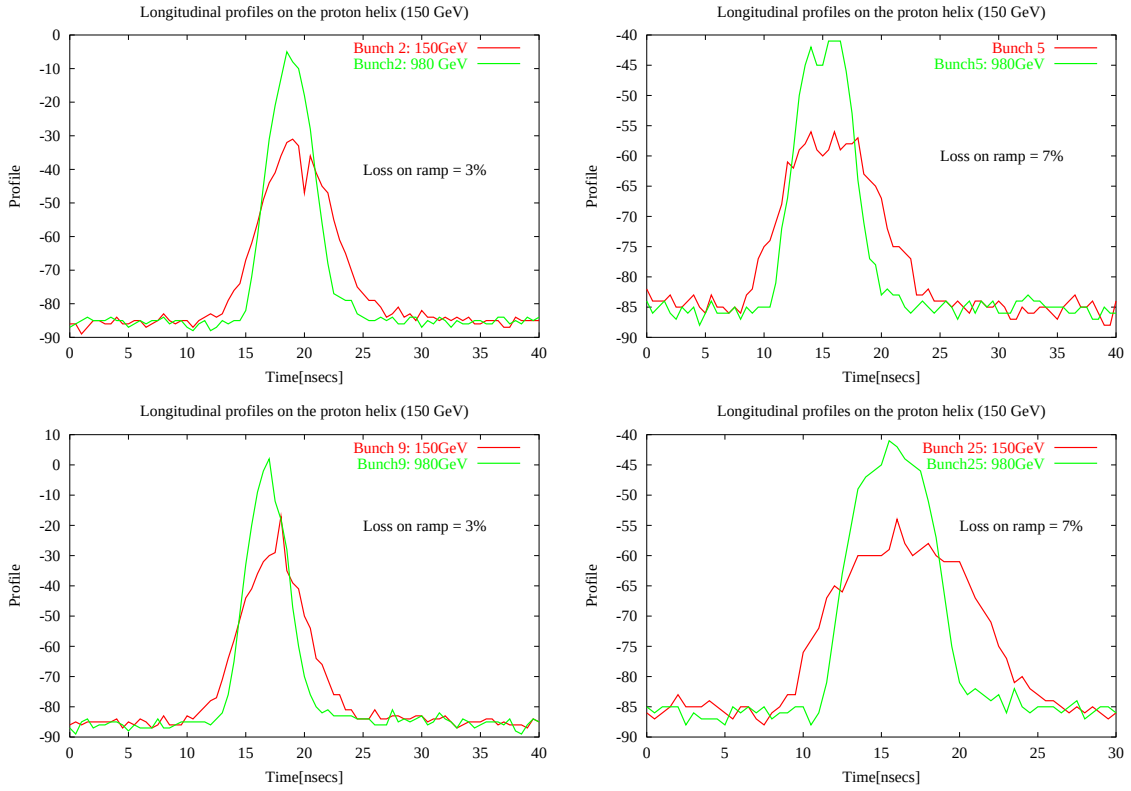

Figure 2.10: (color) Longitudinal profiles of bunches 2, 5, 9 and 25 shown at 150 Gev on the proton helix before the ramp and at 980 GeV after the ramp. The narrower more "Gaussian-like" bunches suffer less loss on the ramp.

Figure 2.10 shows the instantaneous longitudinal profiles of 4 bunches measured on the proton helix, once at 150 GeV and then again at 980 GeV. Bunches 2 and 9 had relatively high intensities of 220×10^9 (as measured in the MI) while bunches 5 and 25 had lower intensities of 170×10^9 (in the MI). The lower intensity bunches 5 and 25 suffered larger losses during the ramp.

This shows clearly that wider longitudinal profiles cause greater losses - the multiple peaks especially at 150 GeV indicate that the bunches were oscillating in the bucket. By contrast, bunches 2 and 9 have profiles closer to a Gaussian and fewer multiple peaks.

The most dramatic difference in transmission loss is between bunches 26 and 27 seen in Figure 2.11. They had similar intensities (180×10^9 in the MI). Bunch 26 was longer and presumably oscillating. It suffered the largest loss $\sim$ 10% amongst all bunches during the ramp. Bunch 27 was shorter but also had a smooth profile without multiple peaks. This bunch had the lowest loss $<$ 3%.

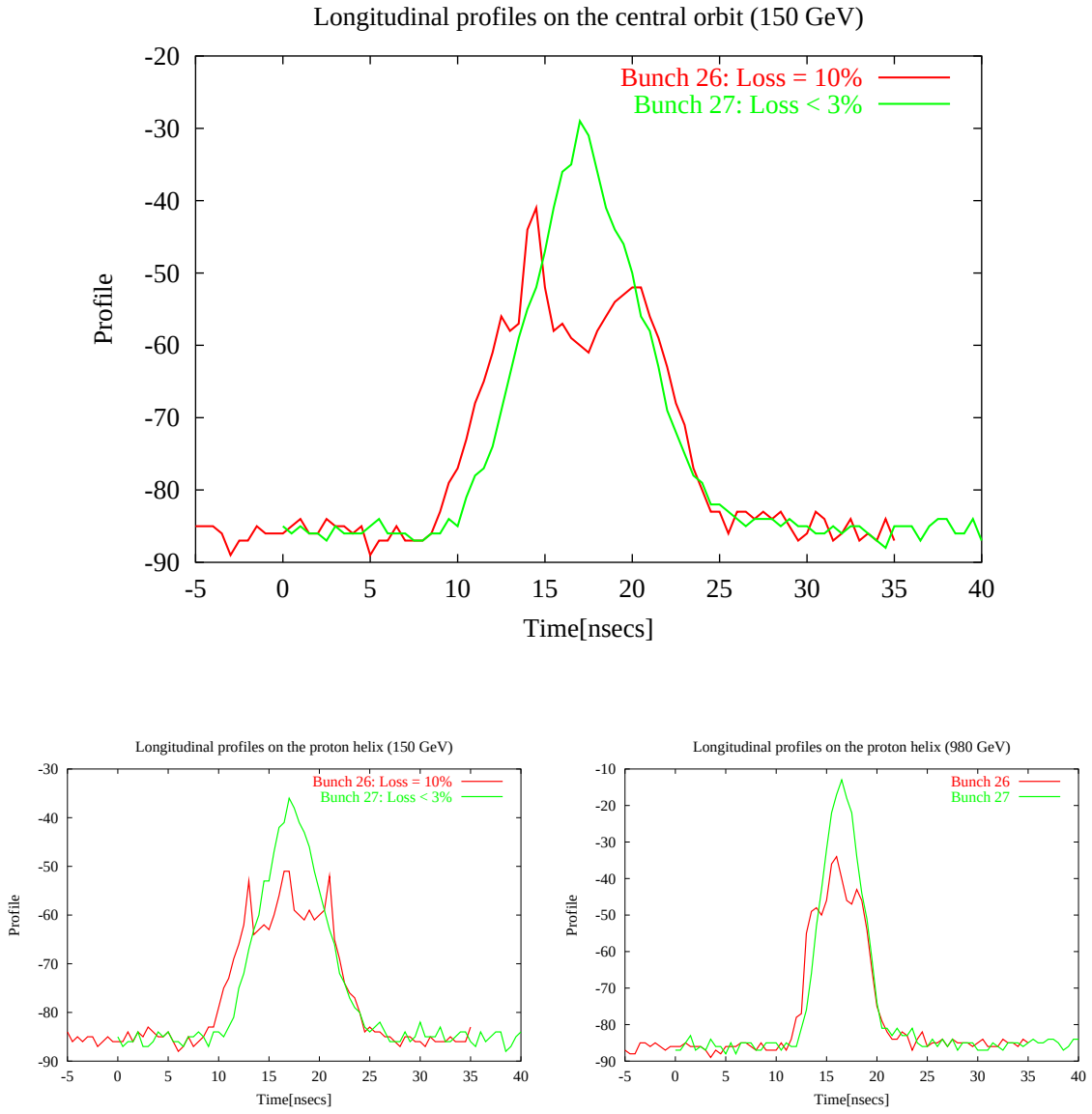

Figure 2.11: (color) Longitudinal profiles of bunches 26 and 27 measured on the central orbit (top), on the proton helix at 150 GeV (bottom, left) and on the helix at 980 GeV (bottom, right). These two bunches had the same intensity. The profile indicates that bunch 26 which lost 10% of its intensity was also oscillating longitudinally.

Figure 2.12 shows further evidence that the losses are determined by the initial longitudinal emittance and profile at the start of the ramp. This plot shows the loss as a function of the change in the longitudinal emittance between the start and the end of the ramp. Since the longitudinal emittance $\epsilon_s \propto \sigma_s^2\sqrt{E}$, we calculate the change in longitudinal emittance from the bunch length reported by the device SBDPSS and the energy ratio from ERING. All bunches whose emittance shrunk by more than 10% ($\Delta\epsilon_s/\epsilon_s < -0.1$) suffered losses greater than 5%. The correlation between the loss and the change $\Delta\epsilon_s$ is also significant $R^2 \sim 0.56$. We conclude that *longitudinal scraping is largely responsible for the beam loss.*

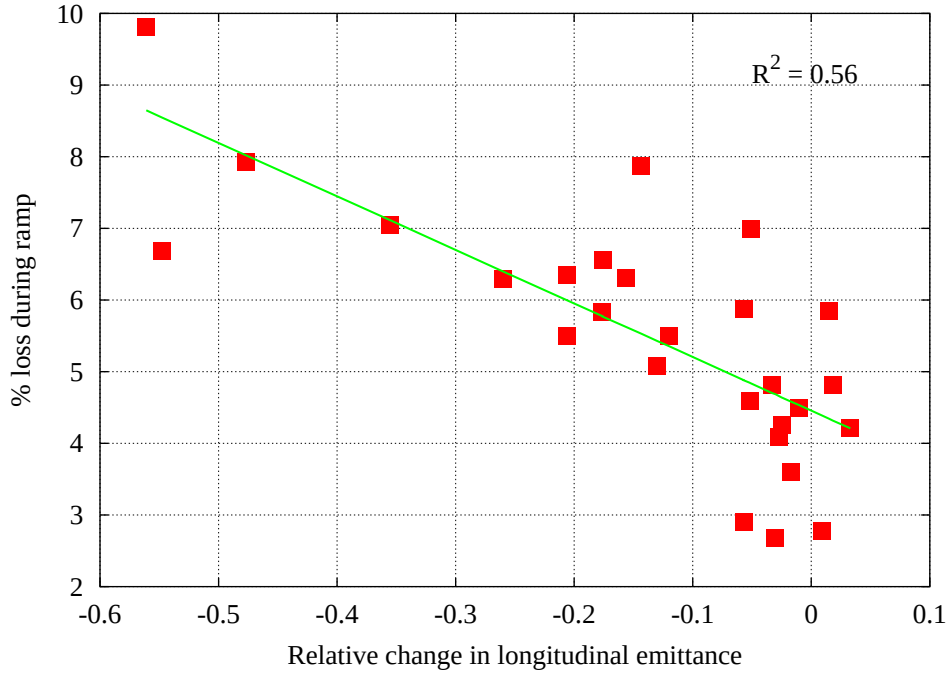

Figure 2.12: Ramp loss vs the change in longitudinal emittance from the start to the end of the ramp.

2.2 Beam loss during the squeeze

Beam losses also occur at other parts of the operational cycle besides the ramp. Figure 2.13 shows the DC beam current IBEAM and proton losses LOSTP as recorded by the loss monitor at CDF. LOSTP, for example, shows that there were sharp increases in losses when the beam was moved to the helix (around 23.1 hrs), at the start of the ramp (just after 23.6 hrs) and then at the start of the low-beta squeeze. The squeeze sometimes excites coherent motion which could be responsible for the increase in losses. However Figure 2.14 shows on the contrary that the Schottky power in both planes dropped at the start of the squeeze and stayed at low levels. Thus the observed increase in losses during the squeeze was not due to coherent beam motion. It is not clear whether proton losses increase to the levels observed in this study during a squeeze in a regular store. If the losses are observed only with protons in the machine, then this would be a signature of a (beneficial) beam-beam effect on the protons from the anti-protons.

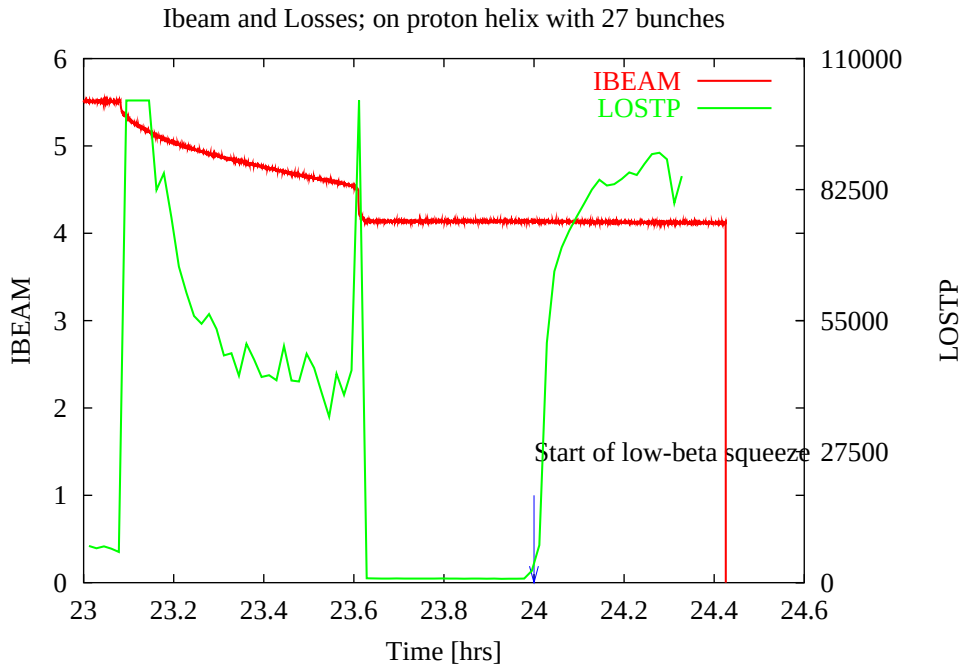

Figure 2.13: (color) The beam current and losses (LOSTP) during the study. The losses rose sharply when the beam was moved to the helix, at the beginning of the ramp and at the start of the low-beta squeeze.

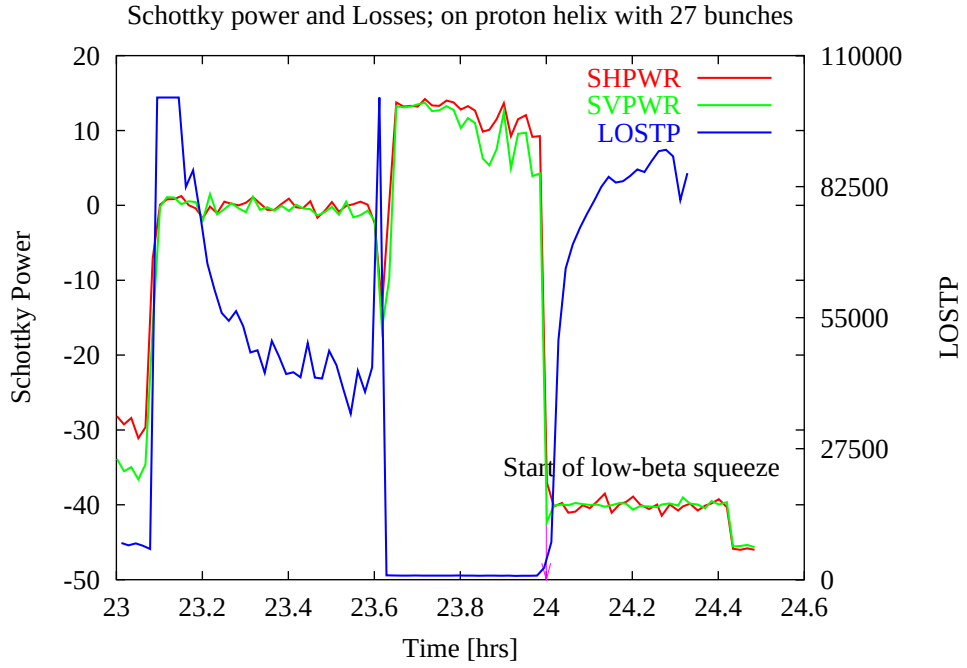

Figure 2.14: (color) Schottky power and proton losses during the study with proton bunches on the proton helix. We observed that while the losses went up by orders of magnitude during the squeeze, the Schottky power decreased by more than 40db and stayed at low levels while the beam was at 980 GeV.

2.3 Protons on the anti-proton helix - analysis

The two proton bunches after being moved to the anti-proton helix were immediately ramped. Figure 2.15 shows the lifetime at the start of the ramp and the loss on the ramp vs bunch intensity. It is evident that there is a negative correlation of these loss parameters with the intensity. Figure 2.16 shows the profile of these bunches at 980 GeV. The bunch length of the less intense bunch P12 was larger than that of P1 and it suffered a somewhat larger loss. The data from these bunches implies that the losses during the ramp on the anti-proton helix are also well correlated with the longitudinal profile and the bunch length.

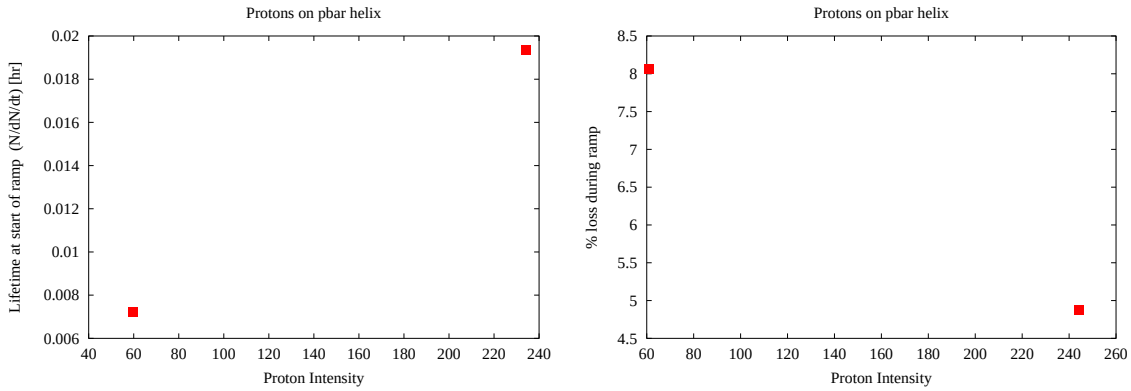

Figure 2.15: Left: Lifetime at the start of the ramp vs bunch intensity; Right: Loss on the ramp vs bunch intensity.

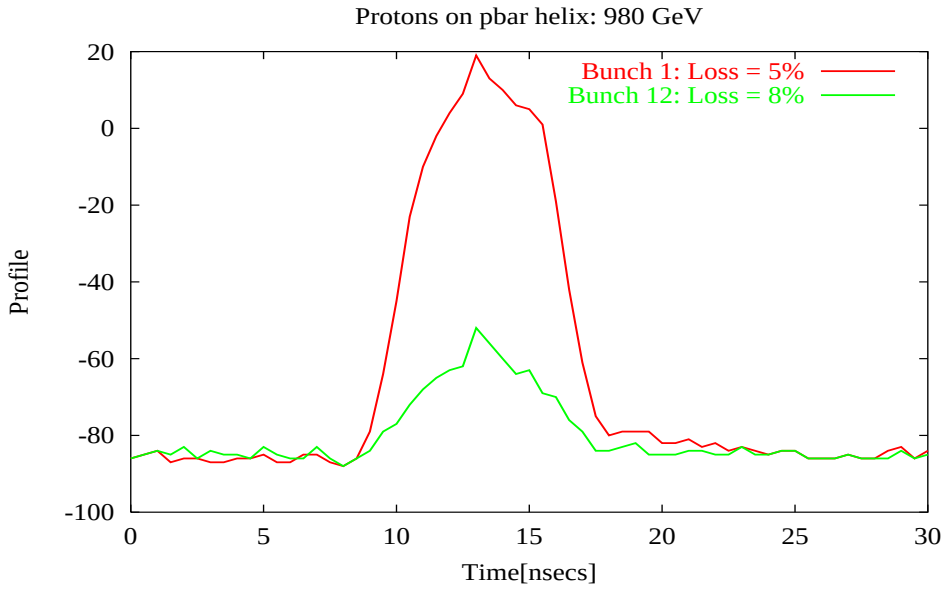

Figure 2.16: (color) Longitudinal profiles of the two bunches at the end of the ramp.

3 Experiment of September 24, 2002

In this experiment we injected an uncoalesced beam as well as 31 coalesced bunches with differing intensities and emittances. Specifically we had:

- 1 uncoalesced beam - this beam occupied buckets 1 through 30
- 4 bunches scraped horizontally at F17 to lower intensity
  - Bunches P6 and P7 (bunches in buckets occupied by bunches 6 and 7 in a 36 bunch train of bunches) scraped to 30% intensity of nominal intensity.
  - P8 and P9 scraped to 60% of nominal intensity
- 9 nominal bunches (i.e. 11 Booster turns, 7 coalesced bunches) in P10, P11, P30 to P36.
- Different number of bunches coalesced in the MI:

  P12 and P13: 11 coalesced bunches, P14 and P15: 9 coalesced bunches, P16 and P17: 5 coalesced bunches, P18 and P19: 3 coalesced bunches.
- Different number of Booster turns:

  P20 and P21: 13 Booster turns, P22 and P23: 9 Booster turns, P24 and P25: 7 Booster turns, P26 and P27: 5 Booster turns P28 and P29: 3 Booster turns.

We observed that the bunch lengths (as reported by SBDPSS) in the Tevatron were about 1 nsec longer than those measured in the Main Injector. This was later attributed to to the fact that the Main Injector reports the "true rms" mentioned earlier while SBDPSS reports a Gaussian fit. Another somewhat surprising observation was the small correlation ($R^2 = 0.26$) between the intensity and the bunch length of coalesced bunches, measured right after injection into the Tevatron. This is seen in Figure 3.1.

We did not capture the longitudinal profiles of any of the coalesced bunches but we did have the profiles of the uncoalesced beam from the mountain range display. Figure 3.2 shows the longitudinal profile of the uncoalesced bunch in bucket 1.

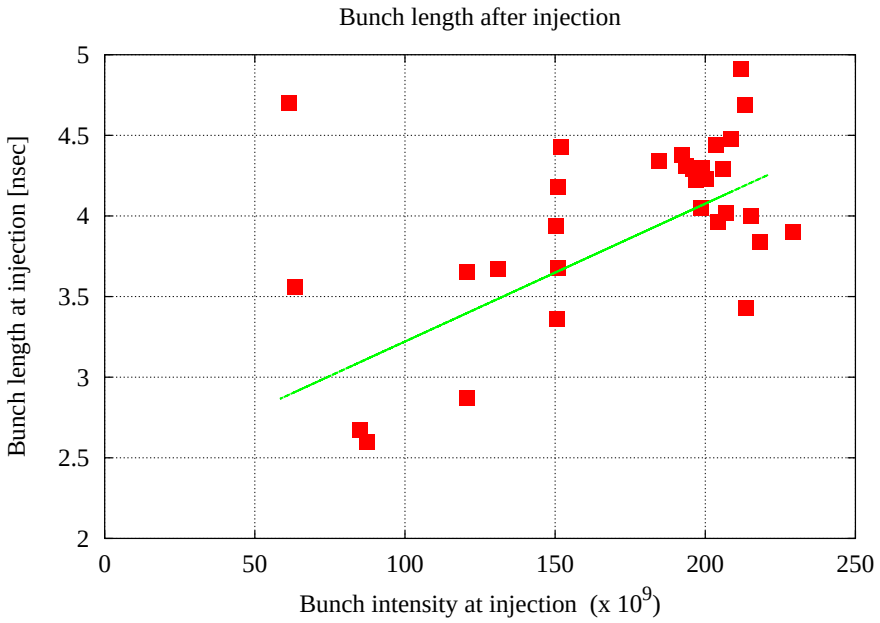

Figure 3.1: Bunch length and intensity of the coalesced bunches. The correlation between the two is not very strong.

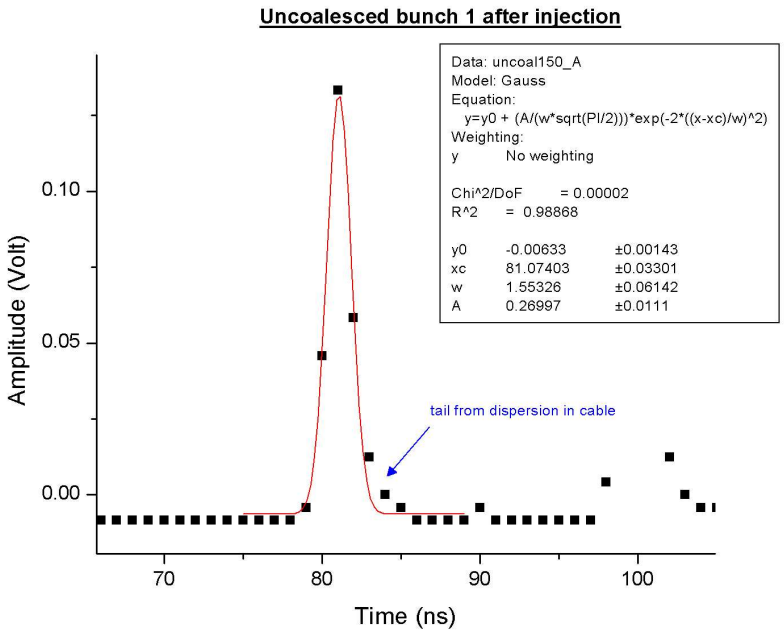

Figure 3.2: Longitudinal profile of the uncoalesced bunch in bucket 1 - obtained from the mountain range display.

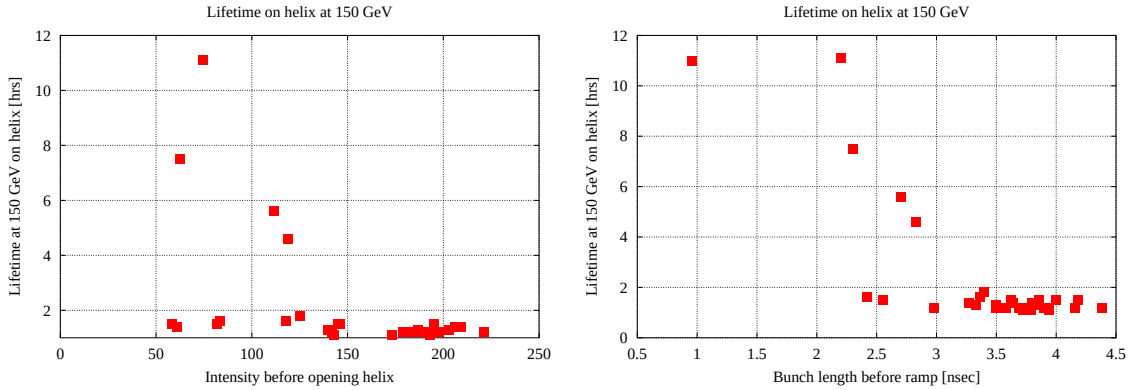

Figure 3.3: Lifetime on the helix at 150 GeV vs Left: bunch intensity; Right: bunch length

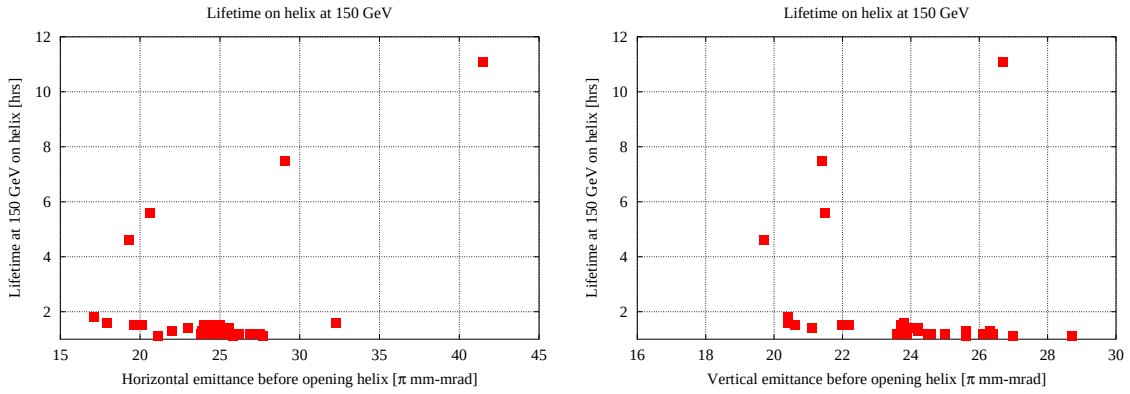

Figure 3.4: Lifetime on the helix at 150 GeV - Left: vs horizontal emittance; Right: vs vertical emittance.

3.1 Lifetime on the helix at 150 GeV

In this experiment, the protons were moved to the proton helix after injection The lifetime on the helix at 150 GeV was observed (by staying at the injection energy for about 15 minutes) and then the beam was ramped. Flying wire measurements of the transverse emittances were taken both before and after the ramp.

The uncoalesced bunches had lifetimes above 11 hours. Most of the coalesced bunches had lifetimes below 2 hours. The exceptions were three of the scraped bunches (P6, P7 and P8) which had lifetimes between 4 and 8 hours. These scraped bunches also had lower longitudinal emittances because they were scraped at a point with high horizontal dispersion. Figure 3.3 shows the lifetime as a function of the intensity and the bunch length - both these quantities shown are the values measured before the beam was moved to the proton helix. The lifetime does not correlate well with the intensity (e.g. bunches with an intensity of 70×10^9 had lifetimes between 1 and 11 hrs). Figure 3.4 shows the dependence of the lifetime on the horizontal and vertical emittances. We observe that the lifetime correlates better with the vertical emittance. For example, for unscraped bunches $R^2 = 0.65$. The correlation is smaller with the horizontal emittance.

We should point out that there are considerable uncertainties with the flying wire measurements of the emittance and not all the measurements make sense. For example, we observed a large drop in the horizontal emittance after beams were moved to the helix but not in the vertical emittance. This is not expected since the major aperture limitation is at C0 in the vertical plane.

3.2 Losses on the ramp

The losses during the ramp differed widely between the bunches. The uncoalesced beam suffered very little loss ($< 2\%$) - close to the resolution of the intensity device. The scraped coalesced bunches also had low losses - between 3 to 5%. Amongst the unscraped bunches, the losses varied between 8 to 12%. We observe that those bunches which had good lifetimes on the helix at 150 GeV also had relatively low losses during the ramp - the correlation between these is $R^2 = 0.74$. Figure 3.5 shows the loss as a function of the intensity before

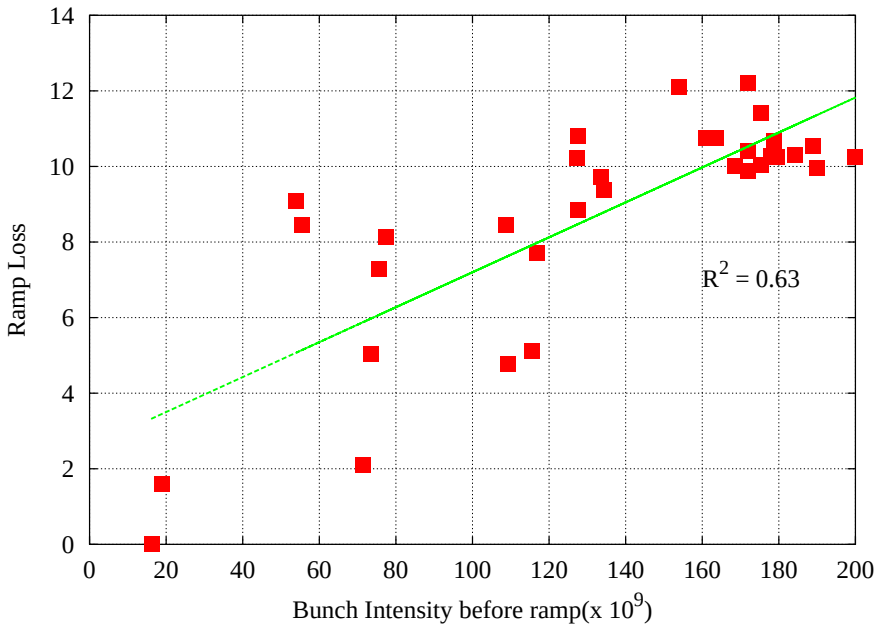

Figure 3.5: Loss on the ramp vs initial intensity.

the ramp. These are reasonably well correlated. However the correlation of the loss with the bunch length before the ramp is much stronger, as seen in Figure 3.6.

If the losses are mainly longitudinal, we expect the bunch area to shrink. Figure 3.7 shows indeed that those bunches whose longitudinal emittance decreased also suffered the largest losses. Bunches whose longitudinal emittance increased had the least loss.

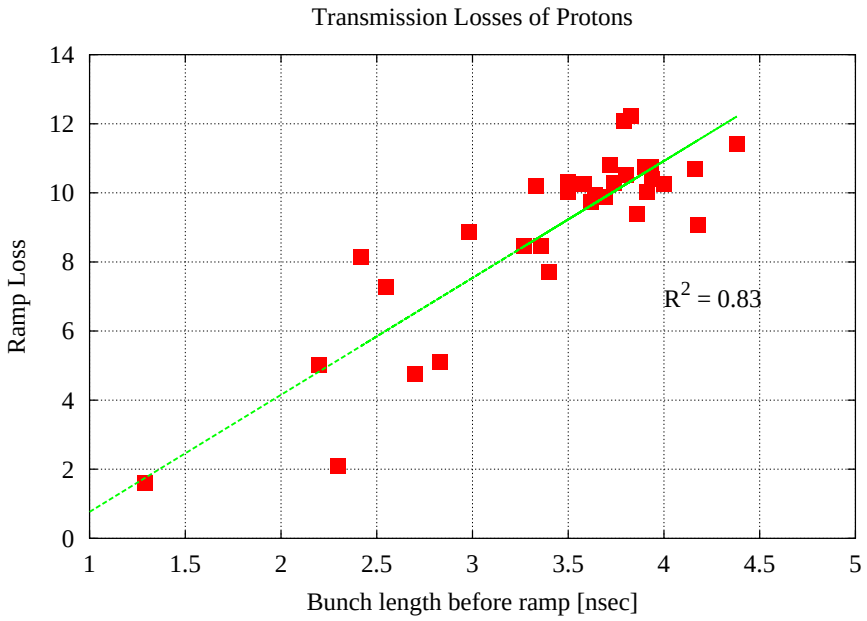

Figure 3.6: Loss on the ramp vs the bunch length before the ramp.

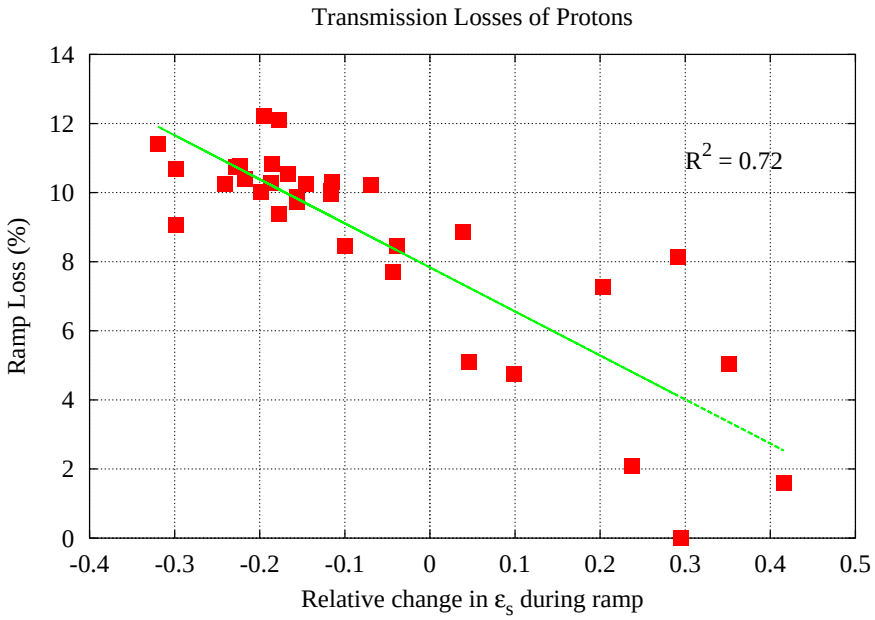

Figure 3.7: Loss on the ramp vs the change in longitudinal emittance after the ramp. The significant correlations $\Rightarrow$ the losses during the ramp are primarily longitudinal in nature.

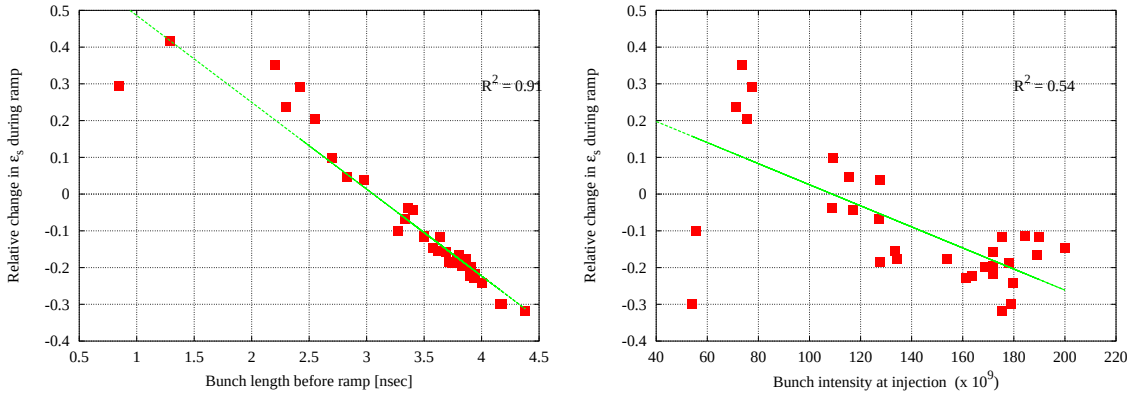

Figure 3.8: Change in longitudinal emittance vs Left: initial bunch length. Right: initial intensity.

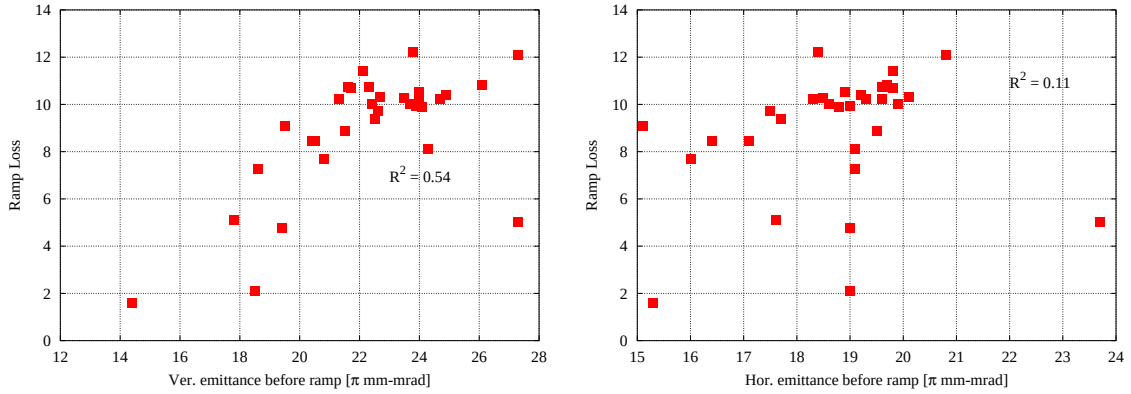

Figure 3.9: Left: Loss on the ramp vs Vertical Emittance; Right: Loss on the ramp vs Horizontal Emittance

The left plot in Figure 3.8 shows that bunches that were longer than 3 nsec had their emittance shrink while those bunches shorter than 3 nsec were able to grow longitudinally within the bucket - the correlation is near perfect as expected. The right plot in Figure 3.8 shows that the change in longitudinal emittance is also somewhat correlated to the intensity - this could be a reflection of the correlation between the intensity and the bunch length. Lastly we examine the correlation of the losses with the transverse emittance - seen in Figure 3.9. There is clearly some correlation with the vertical emittance but almost none with the horizontal emittance.

Table 2 summarizes the correlation of the loss during the ramp with various bunch parameters in decreasing order of importance. Table 3 summarizes the lifetime and ramp loss data for all the different bunch configurations.

	Ramp Loss Correlations R^2			
Bunch parameter	All	All CB	Unscraped CB	Scraped CB
Bunch length just before ramp	0.83	0.68	0.47	0.20
Lifetime on the helix at 150 GeV	0.74	0.64	0.50	0.0
Change in ϵ_s during ramp	0.72	0.63	0.48	0.06
Intensity just before ramp	0.63	0.46	0.48	0.35
Vertical emittance just before ramp	0.54	0.27	0.39	0.12

Table 2: Correlation of the ramp loss with bunch parameters for all bunches, both uncoalesced and coalesced bunches (CB) in decreasing order of importance.

Bunch preparation	Intensity [$\times 10^9$]	Bunch length [nsec]	$\langle \epsilon_V \rangle$ [πmm-mrad]	τ_L on helix [hrs]	Ramp loss %
			Nominal bunches		
	180	3.74	23.8	1.26	11
			Uncoalesced bunches		
	17	2.1	14	> 11	0.8
			Scraped bunches		
Scraped to 60%	112	2.77	18.6	5.1	4.9
Scraped to 30%	72.5	2.25	22.9	9.3	3.6
			Different number of coalesced bunches (CB)		
11 CB	177	3.83	22.0	1.2	10.4
9 CB	168	4.15	21.9	1.2	11.1
5 CB	127	3.16	21.4	1.3	9.5
3 CB	77	2.49	21.5	1.6	7.9
			Different number of Booster turns (BT)		
13 BT	141	3.76	26.7	1.1	11.5
9 BT	174	3.96	23.9	1.4	11.1
7 BT	134	3.74	22.6	1.5	9.6
5 BT	113	3.38	20.7	1.7	8.1
3 BT	55	3.73	20.0	1.5	8.8

Table 3: Average values of the measured intensities, bunch lengths and vertical emittances ϵ_V at the start of the ramp and the measured lifetime τ_L on the helix at 150 GeV and the loss on the ramp.

4 Conclusions

In two dedicated experiments we examined the losses of protons during the ramp. In the first experiment of September 24, 2002 we found that the losses were most strongly dependent on the longitudinal emittance. For example, uncoalesced bunches which had the smallest longitudinal emittance lost less than 2% of their intensity during the ramp. At the other extreme, coalesced bunches with the largest longitudinal emittance lost about 12% of their intensity and furthermore their longitudinal emittance decreased by about 20% after the ramp. This implies that particles from the longitudinal edges were lost. We found a weaker dependence of the loss on bunch intensity and vertical emittance.

In the second experiment on January 6, 2003 we attempted to isolate the dependence of the loss on the individual parameters in a controlled fashion. This time we also obtained the longitudinal profiles of the bunches at 150 GeV both on the central orbit and on the helix and again at 980 GeV. The longitudinal dampers were not turned on so the longitudinal oscillations of the bunches were not damped. We found that the most rapid loss occurs during the first 10 seconds of the ramp when the bucket area is decreasing - see Figure 2.5. Again we found that the loss during the ramp was determined overwhelmingly by the longitudinal emittance and the longitudinal profile. Short coalesced bunches with nearly Gaussian profiles had the smallest losses ($< 2\%$) while long oscillating bunches had losses around 10%. We found very little dependence on the bunch intensity. The same was true when we accelerated two proton bunches on the anti-proton helix.

We conclude that the losses of protons during the ramp can be minimized if the longitudinal emittances are as small as possible and the bunches attain an equilibrium distribution before the start of the ramp. This would require better coalescing in the Main Injector, perhaps with the addition of longitudinal dampers. It might also help to turn on the longitudinal dampers during the ramp in the Tevatron.

Acknowledgments

We thank C. Bhat, D. Capista, I. Kourbanis and S. Pordes for their invaluable help with the experiments.